POLITECNICO DI TORINO
Repository ISTITUZIONALE

An extended and total flux normalized correlation equation for predicting single-collector efficiency

(Article begins on next page)

04 August 2020

An extended and total flux normalized correlation equation for predicting single-collector efficiency

Francesca Messina[1], Daniele Marchisio[2], Rajandrea Sethi[1](*)

[1] *Politecnico di Torino – DIATI – C.so Duca degli Abruzzi 24, 10129 - Torino, Italy*

[2]*Politecnico di Torino - DISAT – C.so Duca degli Abruzzi 24, 10129 - Torino, Italy*

francesca.messina@polito.it, daniele.marchisio@polito.it, rajandrea.sethi@polito.it

(*) Corresponding author:

Dr. Rajandrea Sethi

DIATI - Politecnico di Torino - Corso Duca degli Abruzzi, 24 - 10129 Torino, ITALY

rajandrea.sethi@polito.it. Phone: +390115647735. Fax: +390115647699

Abstract

In this study a novel total flux normalized correlation equation is proposed for predicting single-collector efficiency under a broad range of parameters. The correlation equation does not exploit the additivity approach introduced by Yao et al. (1971), but includes mixed terms that account for the mutual interaction of concomitant transport mechanisms (i.e. advection, gravity and Brownian motion) and of finite size of the particles (steric effect). The correlation equation is based on a combination of Eulerian and Lagrangian simulations performed, under Smoluchowski-Levich conditions, in a geometry which consists of a sphere enveloped by a cylindrical control volume. The normalization of the deposited flux is performed accounting for all of the particles entering into the control volume through all transport mechanisms (not just the upstream convective flux as conventionally done) to provide efficiency values lower than one over a wide range of parameters. In order to guarantee the independence of each term, the correlation equation is derived through a rigorous hierarchical parameter estimation process, accounting for single and mutual interacting transport mechanisms. The correlation equation, valid both for point and finite-size particles, is extended to include porosity dependency and is compared with previous models. Reduced forms are proposed by elimination of the less relevant terms.

Keywords

Colloid transport; particle deposition; porous media; correlation equation; single collector efficiency; nanoparticles

Introduction

Particle transport and deposition in saturated porous media are important processes occurring in natural and engineered systems. Colloidal filtration is a phenomenon of pivotal importance in numerous fields, including the propagation of contaminants and of microrganisms in aquifer systems [1-8] and the clogging of depth filters and wells [9, 10]. Other applications involving particle transport and deposition are: the design of remediation interventions by using nanoparticles as reagents [11-15], the delivery of agents for contrast [16] or for thermo-radiotherapy in medicine [17, 18], enhanced oil recovery or imaging in reservoir engineering [19] and several others [20, 21].

In order to master and control all these applications, a deep understanding of the phenomena involved in particle transport and deposition in saturated porous media is necessary. In this context porous media are described as an ensemble of "collectors" or grains on which the transported particles are collected or deposited. In turn, deposition of particles from a suspension to a collector surface may be viewed as a two-step process: (1) the transport of the particles from the bulk of the suspension to the proximity of the collector and (2) the particle adhesion to the collector/grain surface, which depends on the nature of particle-collector interactions [22]. The first step is usually quantified by η_0, the single collector contact efficiency, that expresses the number of particles that reach the collector divided by the advective rate entering through the projection of the collector (Eq. 3); the second step is commonly quantified by the attachment efficiency α, which is the fraction of the particles coming into contact with the collector that actually attaches onto it. The product of these two values gives, as a result, the single collector removal efficiency η, which accounts for both the transport and attachment steps [23, 24].

According to previous studies, the mechanisms responsible for particle transport are mainly three: Brownian motion, gravity and interception [25] (respectively the blue trajectory AD in Figure 1b, the magenta trajectory G in Figure 1a and the red trajectory AS in Figure 1a). Taking advantage of the additivity concept, Yao et al. [25] firstly proposed in 1971 a correlation equation for the single collector contact efficiency, that is the summation of three partial efficiencies due to Brownian motion η_D, due to gravity η_G, and due to interception η_I. This approach, that neglects the full set of mutual interactions between the different transport mechanisms, reads as follows:

$$\eta_{0\,\text{Yao}} = \eta_D + \eta_G + \eta_I = 4.04 N_{Pe}^{-2/3} + N_G + \frac{3}{2} N_R^{\,2}$$

Eq. 1

where N_{Pe} is the Peclet number, N_G is the gravity number and N_R was defined as the interception number, but in this study for the sake of generalization it will be referred to as steric number or aspect ratio. A detailed definition of these dimensionless numbers is reported in Table 1. It is important to remind here that the additivity is clearly a simplification hypothesis, as the different mechanisms, which are inherently non-linear, operate jointly and therefore neglecting their interactions may lead to large errors.

The first term at the right side of Eq. 1 was derived analytically at high Peclet numbers ($N_{Pe} > 70$) from the results of Levich [26], and takes into account the mutual influence of advection and Brownian motion (or Brownian diffusion). The gravity and interception terms, were analytically calculated by Yao [27], and account respectively for the deposition rate due to gravity and to advection (in this last case for finite-size particles).

Many other more sophisticated correlation equations based on different geometries, such as Happel's and Hemisphere-in-cell, derived by using different numerical approaches (i.e. Lagrangian versus Eulerian) and including more interaction mechanisms (i.e. Van der Waals forces and others) were proposed afterward. Most of them were fully or partially derived starting from the abovementioned additivity assumption.

Rajagopalan and Tien [28] (RT in the figures) extended heuristically the correlation equation presented by Yao et al. [25] by performing a numerical trajectory analysis of non-Brownian particles in the presence of the Van der Waals force and of the hydrodynamic retardation in the Happel's sphere-in-cell model [29]. In 2004 Tufenkji and Elimelech [30] (TE) developed a correlation equation by performing Eulerian simulations in the Happel's geometry and accounting for the simultaneous presence of the transport mechanisms and the effects of the Van der Waals force and of the hydrodynamic retardation [31]. In 2005 Nelson and Ginn [32] adopted a Lagrangian approach in the Happel's geometry, simulating the simultaneous presence of all the forces acting on the particles (i.e. fluid drag, gravity, Van der Waals, electric-double layer, Brownian diffusion and hydrodynamic retardation). Ma et al. [33] (MPFJ) introduced the hemispheres-in-cell model geometry which allows the effect of grain-to-grain contact points to be taken into account. Recently Boccardo et al. [34] solved the full Navier Stokes flow field by exploiting a Eulerian approach and then proposing an extension of the correlation equation for higher Reynolds numbers. As already mentioned, all the above mentioned models are based on the simplification hypothesis of additivity of the three partial efficiencies (η_D, η_G and η_I), as reported in Eq. 1, accounting for two single acting transport mechanisms (gravity and advection) and one mixed term due to the interaction of Brownian diffusion and advection.

As already pointed out by Song end Elimelech [35], Nelson and Ginn [31] and Ma et al. [36], the other main drawback of most of the models is that they overestimate the rate of particle deposition, under some particular conditions. For very small or very big particles and/or for very low approaching velocities, the existing correlation equations predict a single collector contact efficiency higher than one, which is physically questionable [24]. Song and Elimelech [35] analyzed the Happel's-in-cell model and found out that the failure was in the transposition of the boundary conditions from the isolated sphere collector to the sphere-in-cell model: due to the different geometry the same boundary conditions are not correct in the case of very small Peclet numbers. Nelson and Ginn 2011 [31] (NG) proposed a normalized correlation equation, further refined in Nelson et al. 2013 [37], explaining that values above unity are due to an overestimation of η_0 by contributions of diffusion (for small N_{Pe}) and sedimentation (for large N_{Pe}). Ma et al. [36] (MHJ) proposed a normalized correlation equation clarifying that in the case of Lagrangian simulations the prediction of efficiency values greater than one are due to the correlation equations themselves and not to mechanistic trajectory models.

The aim of this study is therefore the development of a novel correlation, that overcomes the two main limitations described above, namely the simplification assumption of additivity, and the overestimation of the collector efficiency (i.e. greater than one) for low approach velocities. This is accomplished by exploiting a hybrid Eulerian-Lagrangian approach for the solution of the colloidal transport problem around a single sphere, by properly accounting for the fact that the different mechanisms operate jointly and interact, and by correctly normalizing the deposition rate with the actual total particle flux entering a control volume. This latter feature ensures efficiency values lower than one, over a broad range of parameters.

Governing equations and numerical simulations

CFD Modeling of Flow and Particle Deposition

Flow and colloidal transport simulations were performed using the finite-elements software COMSOL Multyphisics®. The geometry studied by Yao et al. [25] was recreated in two dimensions under the assumption of axial symmetry, placing a single spherical collector characterized by a radius $a_c = 250 \mu m$ in a cylindical domain 15 times wider and 30 times longer than the collector (Figure 2), in order to minimize the influence of the boundary conditions. Discretization

and meshing were performed using a total number of 249186 triangular and quadrilateral elements ranging from 10^{-8} to 10^{-5} m (see SI).

Stokes flow field was solved numerically by imposing non-slip boundary conditions on the surface of the collector, vertical component of the velocity U at the inlet of the domain and zero pressure at the outlet of the domain.

Point-particles can come into contact with the collector by three mechanisms of transport, namely advection (A), gravity (G), and Brownian diffusion (D). Interception is usually defined as the deposition of a particle which strikes the collector, due to its finite size, while moving along a streamline [23] (AS in Figure 1a). This term is related to the deposition of a finite-size particle in the presence of advective transport only, but in real systems the steric size of the particles can influence the deposition of particles transported by gravity (not just affecting the settling velocity), by Brownian motion (not just through change of diffusion coefficient) and by a combination of the transport mechanisms. Therefore we prefer to refer to the steric effect (S) as the increase of deposition due to finite-size particles, in the presence of any other transport mechanism.

A Lagrangian approach was used only for the null diffusion cases $(D = 0, N_{Pe} \rightarrow \infty)$, which is virtually impossible to simulate with the Eulerian approach, while most other transport simulations were performed in a Eulerian framework, thus numerically solving the advection diffusion equation reported in Eq. 2

$$\nabla \cdot (\mathbf{u}c + \mathbf{V}c) = \nabla \cdot (D\nabla c)$$

Eq. 2

where $\boldsymbol{u}$ is local fluid velocity, $\boldsymbol{V}$ is the velocity induced by the gravity force (Stokes or terminal velocity, defined in Table 1), c is the particle concentration and D is the diffusion coefficient of the suspended particle defined in Table 1. Inlet concentration was set equal to C_0 and a perfect sink scenario was simulated by placing an assigned $c=0$ concentration on the surface of the collector for point-particles (or at distance a_p from the surface of the sphere to account for steric effect associated with finite-size particles). In order to recreate the scenario proposed by Yao et al. [25], London van der Waals and the hydrodynamic interactions between particles and the solid wall were neglected. This choice is coherent with the Smoluchowski–Levich approximation which assumes that hydrodynamic retardation experienced by the particle is balanced by the London Van der Waals forces between particles and collector [22, 23, 38]. This approximation holds true when particle dimension is less than the particle diffusion boundary layer [34, 39] (which is always in the micrometer range for the simulations performed).

The simulations were performed over a wide range of variation of non-dimensional parameters involved in the problem as reported in Table 1: the values were chosen with a logarithmic pattern. A comparison with the range of values that these non-dimensional parameters typically assume in aquatic systems is reported in Table S2 of the SI. A total of 200 Lagrangian and 1320 Eulerian simulations were performed.

Numerical Calculation of Normalized Single Collector Contact Efficiency

Previous studies determined the single collector contact efficiency as the ratio between the overall rate of particle collisions with the collector I_s, calculated by integrating the particle flux over the entire surface of the sphere, and the advective particle flux entering the projected area of the collector [25, 30] (Eq. 3) or through the fluid envelope (by introducing the correction factor γ^2, see Logan et al. [40] for detailed information and also the SI, Eq. S3).

$$\eta_0 = \frac{I_s}{\pi a_c^2 U C_0}$$

Eq. 3

In the framework of this study, we performed mass balance over a cylindrical control volume (with its radius incremented by a_p in case of finite-size particles to account for steric effect) tangent to the spherical collector. We propose a *total flux normalized* single collector contact efficiency (Eq. 4) as the ratio between the rate of particle colliding with the collector I_s divided by the total rate of particles I_c entering by advection, gravity and diffusion into the cylindrical control volume. The contribution of advection and gravity fluxes is predominant at the top of the cylindrical surface; conversely, diffusion is usually the dominant flux through the lateral wall of the cylinder (Figure 2).

$$\eta_N = \frac{I_s}{I_c}$$

Eq. 4

In this way the denominator of Eq. 4 is always greater than or equal to the one present in the definition of η_0 (Eq. 3). I_c is not only the advective flux coming from a limited part of the domain (as the projection of the collector), but it represents the total flux that could potentially deposit on the collector, thus it is always greater than or equal to I_s. In fact, I_c includes also (i) the effect of other transport mechanisms (gravity and diffusion) acting on the particles, (ii) lateral fluxes contributing to the movement of particles toward the collector and (iii) an increased area of the top

7

projection of the sphere whose radius is increased by a_p to rigorously account for the finite size of the particles $\left(\pi\left(a_c+a_p\right)^2\right)$.

General Formulation of the Novel Correlation Equation

In the *total flux normalized* correlation equation the rate of particle collisions with the collector I_s and the total rate of particles entering into the cylinder I_c are expressed as a summation of seven terms (Eq. 5). As can be inferred from Eq. 6 each term is composed by the sum of two power functions: the first depends on the transport mechanisms i.e. by their characteristic velocities $\left(U,V,D/(2a_c)\right)$ and the second depends also on the steric contribution induced by the finite-size of the particles and therefore on N_R. Multiplication by the surface of the projection of the sphere $\left(\pi a_c^2\right)$ was performed in order to more easily compare the proposed model with the results of previous studies. The seven terms reported in Eq. 5 are therefore due to single and mutually interacting transport mechanisms and the steric effect:

- terms 1-3 depend on one transport mechanism (advection (A), gravity (G) or diffusion (D)) which acts alone, through its characteristic velocity (respectively $U,V,D/(2a_c)$), with or without steric contribution N_R (S);

- terms 4-6 depend on two combined transport mechanisms (AG, AD, DG) and therefore simultaneously on two characteristic velocities and on steric contribution;

- term 7 depends on the mutual presence of the three combined mechanisms (ADG) and therefore on all the three characteristic velocities and on steric contribution .

$\alpha_i,\beta_i,\gamma_i,k_{s1,i}$ and $k_{s2,i}$ are the exponents and the coefficients that need to be estimated by the fitting procedure.

For non-null advection, in order to compare the proposed correlation equation to previous formulations, it is possible to arbitrarily divide I_s and I_c by the denominator of η_0 (i.e. the advective rate passing through the top of the cylinder $\pi a_c^2 U C_0$) thereby obtaining Eq. 7. This equation depends on the non-dimensional numbers N_{Pe},N_G and N_R. In this way, the numerator of the normalized efficiency (Eq. 7) can clearly be considered an extended formulation of Yao's η_0 (Eq. 8).

$$\eta_N = \frac{I_s}{I_c} = \frac{I_{s,1}^{A,S} + I_{s,2}^{G,S} + I_{s,3}^{D,S} + I_{s,4}^{AG,S} + I_{s,5}^{AD,S} + I_{s,6}^{DG,S} + I_{s,7}^{AGD,S}}{I_{c,1}^{A,S} + I_{c,2}^{G,S} + I_{c,3}^{D,S} + I_{c,4}^{AG,S} + I_{c,5}^{AD,S} + I_{c,6}^{DG,S} + I_{c,7}^{AGD,S}}$$

Eq. 5

$$I_s = \pi a_c^2 C_0 \sum_{i=i}^{7} U^{\alpha_i} V^{\beta_i} \left(\frac{D}{2a_c} \right)^{1-\alpha_i-\beta_i} \left(k_{s1,i} + k_{s2,i} N_R^{\gamma_i} \right)$$

$$I_c = \pi a_c^2 C_0 \sum_{i=i}^{7} U^{\alpha_i} V^{\beta_i} \left(\frac{D}{2a_c} \right)^{1-\alpha_i-\beta_i} \left(k_{c1,i} + k_{c2,i} N_R^{\gamma_i} \right)$$

Eq. 6

$$\eta_N = \left. \frac{I_s}{I_c} \right|_{U \neq 0} = \frac{\sum_{i=i}^{7} N_G^{\beta_i} N_{Pe}^{\alpha_i+\beta_i-1} \left(k_{s1i} + k_{s2i} N_R^{\gamma_i} \right)}{\sum_{i=i}^{7} N_G^{\beta_i} N_{Pe}^{\alpha_i+\beta_i-1} \left(k_{c1i} + k_{c2i} N_R^{\gamma_i} \right)} = \frac{\eta_0}{\sum_{i=i}^{7} N_G^{\beta_i} N_{Pe}^{\alpha_i+\beta_i-1} \left(k_{c1i} + k_{c2i} N_R^{\gamma_i} \right)}$$

Eq. 7

$$\eta_0 = \frac{I_s}{\pi a_c^2 U C_0} = \eta_0^A + \eta_0^{AS} + \eta_0^G + \eta_0^{GS} + \eta_0^D + \eta_0^{DS} + \eta_0^{AG} + \eta_0^{AGS} + \eta_0^{AD} + \eta_0^{ADS} + \eta_0^{DG} + \eta_0^{DGS} + \eta_0^{AGD} + \eta_0^{AGDS}$$

Eq. 8

Fitting and Parameter Estimation

The fitting of the coefficients $\left(k_{s1,i} \text{ and } k_{s2,i} \right)$ and exponents $\left(\alpha_i, \beta_i \text{ and } \gamma_i \right)$ was perfomed by simultaneously minimizing the sum of the residual between the CFD data of deposition I_s, of the rate of particles entering the cilinder I_c and of the normalized efficiency η_N and their correspondent models (Eq. 5 and Eq. 6); (further details are presented in the SI). The parameter estimation was performed using a hierarchical procedure which begins from point-particles by determing the coefficients and exponents corresponding to only one transport mechanism, thus when two transport mechanisms are absent (first level in Figure 3). Subsequently, the coefficients and exponents for couples of combined mechanisms acting together, (therefore when at least one transport mechanism is absent, second level in Figure 3) were estimated. Finally, the parameters of three combined transport mechanisms were determined (third level in Figure 3). The procedure was then repeated in order to estimate the coefficients for finite-size particles (considering the steric effect).

The simultaneous fitting of the rates and of the efficiency was adopted in order to improve and regularize the fitting procedure. The hierarchical procedure is necessary to guarantee the full independence of the fitting results when any of the transport mechanisms is removed. Otherwise, a global fitting on all the data set (such as those conducted in some of the previous studies) would have provided coefficients that were always indirectly dependent on the mutual presence of all the transport and steric effect mechanisms acting together [32], thus biasing the results.

Results and Discussion

Overall Normalized Correlation Equation for Single-Collector Contact Efficiency

The coefficients of the proposed correlation equation (reported in Table 2) were derived by applying the fitting procedure described in the previous paragraph to the data obtained from the CFD numerical simulations leading to Eq. 9 and Eq. 10, which are valid in case of not null advection. (The relationships are implemented in an Excel spreadsheet that can be downloaded from http://areeweb.polito.it/ricerca/groundwater/software/ETAMMS2015.html).

$$\eta_N = \eta_0 / \left[\left(1 + 6.0098 N_R^{1.9834}\right) + N_G \left(1 + 6.0187 N_R^2\right) + N_{Pe}^{-1} \left(7.5609 + 4.9534 N_R^1\right) + N_G^{0.8741} \left(0.0442 + 0.1220 N_R^{0.4210}\right) \right.$$
$$\left. + N_{Pe}^{-0.6338} \left(2.9352 + 2.7480 N_R^{0.3737}\right) + N_G^{0.6550} N_{Pe}^{-0.3450} \left(2.7972 + 3.4372 N_R^{0.6012}\right) + N_G^{0.5873} N_{Pe}^{-0.2565} \left(-1.1945 - 1.2616 N_R^{0.5438}\right) \right]$$

Eq. 9

$$\eta_0 = 1.5062 N_R^{1.9834} + N_G \left(1 + 6.0187 N_R^2\right) + N_{Pe}^{-1} \left(7.5609 + 4.9534 N_R^1\right) + N_G^{0.8741} \left(0.0442 + 0.1220 N_R^{0.4210}\right) +$$
$$+ N_{Pe}^{-0.6338} \left(2.9352 + 2.7480 N_R^{0.3737}\right) + N_G^{0.6550} N_{Pe}^{-0.3450} \left(0.9461 + 1.1626 N_R^{0.6012}\right) + N_G^{0.5873} N_{Pe}^{-0.2565} \left(-0.6740 - 0.7119 N_R^{0.5438}\right)$$

Eq. 10

Because of the assumptions used for the numerical simulations, the results are valid under the conditions of creeping flow field and in the absence of external forces except gravity. In particular, the Smoluchowski-Levich assumption was used and therefore the Van der Waals interactions and the hydrodynamic retardation were neglected. A calibration plot showing the excellent agreement between the efficiency derived from numerical simulations and the correlation equation of η_N, over the wide and full set of data, is shown in Figure 4. In Figure 5 the proposed normalized correlation equation of η_N is compared to numerical data calculated for typical values of engineering applications.

Unique Features of the Normalized Correlation Equation and Comparison with Previous Results

From the parameters listed in Table 2 the following considerations can be drawn:

- since k_{s1}=0, the advection contributes, coherently with previous models, to the rate of deposition on the collector only in the presence of the particle finite-size effect, i.e. when interception (the advection associated with the steric effect) is not negligible;

- the sum of the three exponents of the transport velocities is equal to one for every term, coherently with dimensional analysis;

- the mixed terms account for mutual interaction among transport mechanisms, including also the steric effect;

- the presence of other terms at the denominator of the expression for η_N allows normalization of the efficiency also when advection is not the dominant transport mechanism and in particular at high N_G and low N_{Pe} conditions. The value of η_N is less than or equal to one in all the simulated domain and also in limiting conditions (e.g. $U,V,D \rightarrow 0,\infty$);

- previous studies have argued that the three terms present in the model proposed by Yao et al. [25] are due to the transport mechanisms of diffusion, gravity and interception. Analysing the extended formulation of η_0 here proposed, it is possible to note that the three terms introduced by Yao et al. [25] in Eq. 1 actually correspond to the mechanisms of: advection and steric effect (interception) ($i=1$, η_0^{AS}, AS in Figure 1a), gravity ($i=2$ with $k_{s2}=0$, η_0^{G}, G in Figure 1a) and advection and diffusion ($i=5$, with $k_{s2}=0$, η_0^{AD}, AD in Figure 1b). As a matter of fact the term usually called η_D is actually the rate of attachment due to the mix processes of advection and diffusion, divided by the advection rate passing through the projection of the sphere $\eta_0^{AD} = \dfrac{I_{s,5}^{AD}}{I_{c,1}^{A}}$. This conclusion agrees with the assumption adopted by Levich [26] in deriving the total particle flux on a sphere at high N_{Pe} numbers (i.e. $N_{Pe} > 70$), a result later used by Yao for the calculation of the expression $N_{Pe}^{-2/3}$. The value of $k_{s1,5}$ derived in our expression is different from those proposed in previous studies due to the presence of a further term accounting only for diffusion as a transport mechanism $I_{s,3}^{D}$. The term η_G is $\eta_0^{G} = \dfrac{I_{s,2}^{G}}{I_{c,1}^{A}}$ and therefore is exactly the ratio between the rate of

11

deposition due to the sole gravity and the advective rate through the top of the cylinder. Finally the interception term η_I is due to advection and steric effect and it is equal to $\eta_0^{AS} = \dfrac{I_{s,1}^{A,S}}{I_{c,1}^{A}}$;

- the novel correlation equation provides consistent results also for point particles (i.e. $N_R \rightarrow 0$);

- the total flux normalized equation provides values lower than one also for limiting conditions (Figure 6B);

- the formulation provides consistent results also when one or two transport mechanisms are absent (since some single or mixed terms are disappearing).

Comparison with Other Correlation Equations

A comparison with previous correlation equations was attempted under two conditions:

- high porosities ($n \rightarrow 1$): this is the natural condition for the comparison of the different models since, for porosities approaching to one, they all produce a single collector in a pseudo-infinite domain (e.g. Yao's domain). In this case the normalizing flux (advective or total) is calculated over the projection of the collector $\left(\pi a_c^2 \right)$.

- realistic porosities: in order to compare the models over a wide range of porosities and to normalize the efficiencies accounting for the fluxes entering the fluid enveloped $\left(\pi b^2 \right)$, the *porosity-dependent parameters* $\gamma = (1-n)^{1/3}$ and A_s were introduced in Eq. 9 and Eq. 10 leading to Eq. 11 and Eq. 12 (further details are reported in the SI).

$$\eta_{N,\gamma} = \eta_{0,\gamma} / \left[\left(1 + A_S 6.0098 N_R^{1.9834} \right) + N_G \left(1 + 6.0187 N_R^2 \right) + \gamma^2 N_{Pe}^{-1} \left(7.5609 + 4.9534 N_R^1 \right) / (2 - 2\gamma) + \right.$$
$$+ A_S^{0.1259} N_G^{0.8741} \left(0.0442 + 0.1220 N_R^{0.4210} \right) + A_S^{0.3662} N_{Pe}^{-0.6338} \left(2.9352 + 2.7480 N_R^{0.3737} \right) +$$
$$\left. N_G^{0.6550} N_{Pe}^{-0.3450} \left(2.7972 + 3.4372 N_R^{0.6012} \right) + A_S^{0.1562} N_G^{0.5873} N_{Pe}^{-0.2565} \left(-1.1945 - 1.2616 N_R^{0.5438} \right) \right]$$

Eq. 11

$$\eta_{0,\gamma} = \gamma^2 \left[1.5062 A_S N_R^{1.9834} + N_G \left(1 + 6.0187 N_R^2 \right) + N_{Pe}^{-1} \left(7.5609 + 4.9534 N_R^1 \right) / (2 - 2\gamma) + \right.$$
$$+ A_S^{0.1259} N_G^{0.8741} \left(0.0442 + 0.1220 N_R^{0.4210} \right) + A_S^{0.3662} N_{Pe}^{-0.6338} \left(2.9352 + 2.7480 N_R^{0.3737} \right) +$$
$$\left. + N_G^{0.6550} N_{Pe}^{-0.3450} \left(0.9461 + 1.1626 N_R^{0.6012} \right) + A_S^{0.1562} N_G^{0.5873} N_{Pe}^{-0.2565} \left(-0.6740 - 0.7119 N_R^{0.5438} \right) \right]$$

Eq. 12

From the plots shown in Figure 6, it is possible to state that the novel η_0 can be compared to the previous proposed equations normalized over the advective flux (namely, Yao, TE, MPFJ), which provide efficiencies higher than one under low N_{Pe} and high N_G conditions both for unity and realistic porosities. The Rajagopalan and Tien [28] (RT) equation corrected by Logan et al. [40] produces values different from the other equations at high porosity values. On the contrary η_N generates values always lower than one over the entire range of parameters. Under gravity dominating conditions it produces an asymptote which is equal to one for $n=1$ and lower than one for realistic porosities, in accordance with previous models (NG and MHJ). For pure diffusion (low N_{Pe}) the proposed correlation tends asymptotically to one without showing any local maximum. This behavior is different from those presented in previous models by NG and MHJ, showing respectively values above unit (as stated in Nelson at al. [37]) and a local maximum at increasing N_{Pe} (see Figure 6 IIB)). The absence of a local maximum in the MMS model can be explained by the presence of additional terms both at the numerator and at the denominator of the proposed formula, in particular by the presence of a pure diffusion term $I_{s,3}^D$ which is not present in previous correlation equations. The numerical simulation results point out the absence of a local maximum as shown in Figure S6 in the SI, where deposition efficiency for small particles is reported.

In the SI further comparisons are presented including the London Van der Waals force implementation in previous correlation equations. Figure S5 (in the SI) shows that our correlation equation generates robust results over a wide range of parameters even if it was derived under the Smoluchowski-Levich approximation.

Reduced Models

Figure 7 shows the effect on the fitting residual when a single or a combination of mechanisms is removed from Eq. 9. The best fit of the numerical simulations in a pseudo infinite domain is obtained when all the mechanisms are acting with all the possible combinations leading to a residual of 0.23 (full η_N). As expected, the three terms included in the Yao et al. [25] model are the most important ones (advection term is obviously fundamental and present only at the denominator), but also pure diffusion is a key term.

Several reduced models for the total flux normalized correlation equation can be proposed by eliminating the less important terms in Eq. 9. In particular a reduced model providing a residual of 0.53 can be obtained including, both at the numerator and at the denominator, the mechanisms of A, G, AS, AD, D, DG, ADS. Eq. 13 shows the reduced model of η_N including the porosity dependency.

Furthermore, the extended expression of η_0 provides a residual of 0.38 if compared to numerical values derived from CFD simulations. Keeping only the terms present in the Yao equation (A, G, AS, AD) leads to a residual of 36.09 that reduces to 5.09 if the same mechanisms reported above are included (i.e. A, G, AS, AD, D, DG, ADS). The reduced model, extended to include porosity dependency, is reported in Eq. 14. These two reduced models are consistent with the efficiency definition presented in Eq. S3 (SI), which normalizes the fluxes on the fluid envelope of the Happel's model.

$$
\eta_{N,\gamma}^R = \eta_{0,\gamma}^R / \Big[\big(1 + 6.0098 A_S N_R^{1.9834}\big) + \gamma^2 7.5609 N_{Pe}^{-1} / (2 - 2\gamma) + N_G + \\
+ A_S^{0.3662} N_{Pe}^{-0.6338} \big(2.9352 + 2.7480 N_R^{0.3737}\big) + 2.7972 N_G^{0.6550} N_{Pe}^{-0.3450} \Big]
$$

Eq. 13

$$
\eta_{0,\gamma}^R = \gamma^2 \Big[1.5062 A_S N_R^{1.9834} + 7.5609 N_{Pe}^{-1} / (2 - 2\gamma) + N_G + A_S^{0.3662} N_{Pe}^{-0.6338} \big(2.9352 + 2.7480 N_R^{0.3737}\big) + 0.9461 N_G^{0.6550} N_{Pe}^{-0.3450} \Big]
$$

Eq. 14

It is important to note that both the full and reduced models, that we derived (a comparison is shown in Figure 8), include a term which accounts for pure diffusion, scaling with N_{Pe}^{-1}. This term is not present in the Yao et al. [25] equation, but it is of pivotal importance in order to extend the correlation equation to low Peclet regime (i.e. $N_{Pe} < 70$). This conclusion is consistent with the study by Prieve and Ruckenstein [39] and Ma et al. [36].

Conclusions

In this study a novel total flux normalized correlation equation (i.e. less than or equal to one in any conditions) for predicting single-collector efficiency was derived by means of a mass balance acting on a cylindrical domain including the collector. The proposed correlation equation is not derived by exploiting the additivity concept proposed by Yao et al. [25], but includes also mixed terms accounting for the mutual interaction of concomitant transport mechanisms (i.e. advection, gravity and Brownian motion) and steric effect. The correlation equation was extended in order to include porosity dependency and reduced forms were presented including the most relevant interacting mechanisms. In future studies the proposed approach will be further extended to more complex geometry and more particle-collector interactions.

SUPPORTING INFORMATION AVAILABLE

Details on mesh features, the range of dimensionless parameters investigated, the fitting method, the role of porosity are provided in the Supporting Information.

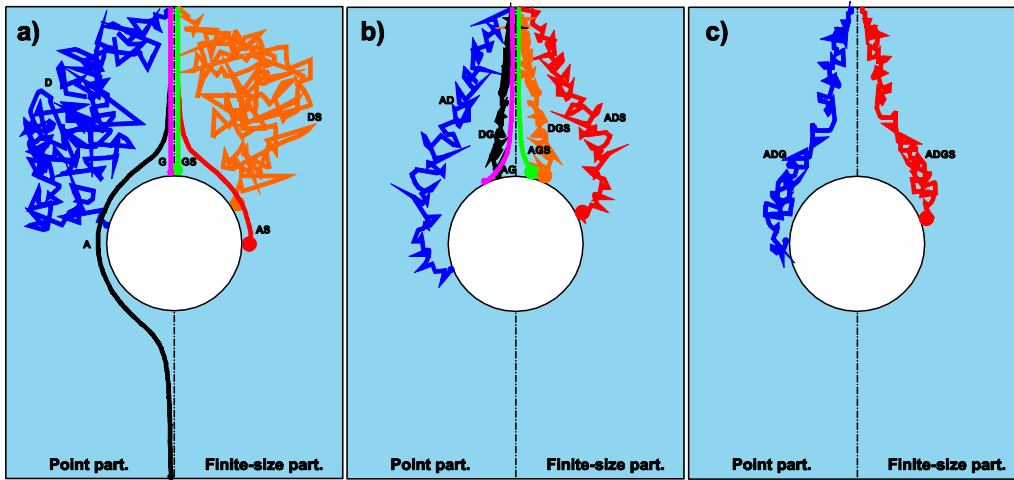An Excel spreadsheet implementing the proposed correlation equations, together with CFD data, can be downloaded from http://areeweb.polito.it/ricerca/groundwater/software/ETAMMS2015.html).

Figure 1: Main mechanisms of particles transport and deposition. (a) Single transport mechanism: diffusion D (blue line), advection A (black line), gravity G (magenta line), diffusion and steric effect DS (orange line), advection and steric effect AS (red line), gravity and steric effect GS (green line); (b) Two active transport mechanisms: diffusion and advection AD (blue line), gravity and diffusion DG (black line), advection and gravity AG (magenta line), diffusion-advection and steric effect ADS (red line), gravity-diffusion and steric effect DGS (orange line), advection-gravity and steric effect AGS (green line); (c) Three transport mechanisms acting together: advection-diffusion and gravity ADG (blue line), advection-diffusion-gravity and steric effect ADGS (red line).
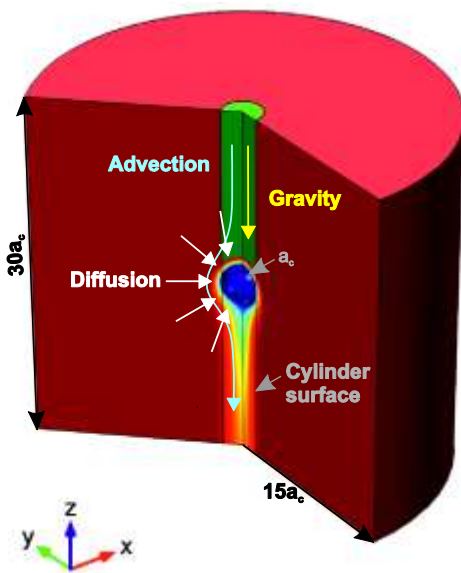

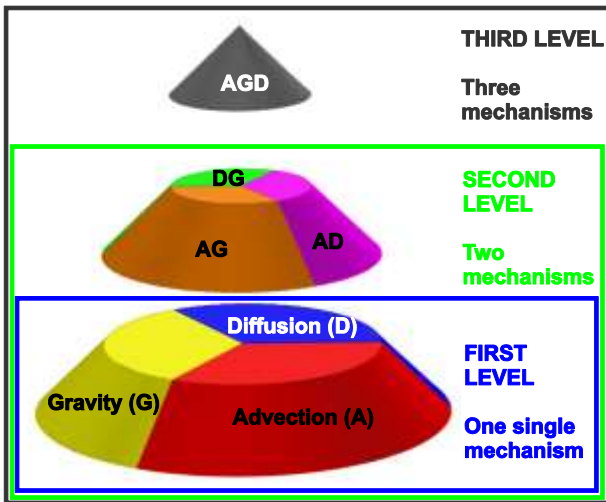**Figure 2: Geometry characteristics of the domain and directions of the main fluxes.**

Figure 3: Schematic representation of the three step interpolation procedure. First level: single transport mechanisms; second level: coupled transport mechanisms; third level: advection, gravity and diffusion acting together.
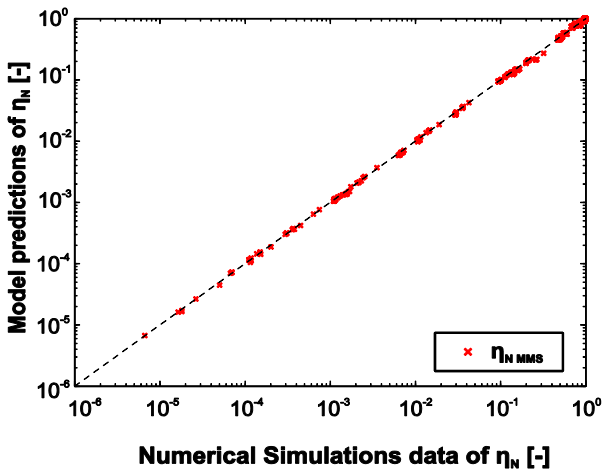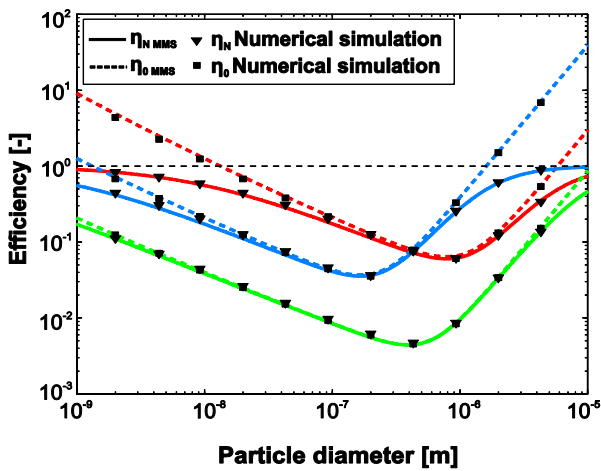

Figure 4: Calibration diagram of η_N .

Figure 5: The proposed correlation equation of η_N (full line) and η_0 (dotted line) and some numerical simulations results (triangles for η_N and squares for η_0). Data: ρ_f =998 kg/m³, T=288 K, μ =9.8·10⁻⁴ Pa·s, a_c=250 µm, U = 1·10⁻⁶ m/s (red lines), 1·10⁻⁵ m/s (blue lines), 1·10⁻⁴ m/s (green lines) and ρ_p = 1050 kg/m³ (red lines), 7800 kg/m³ (blue lines), 2500 kg/m³ (green lines).
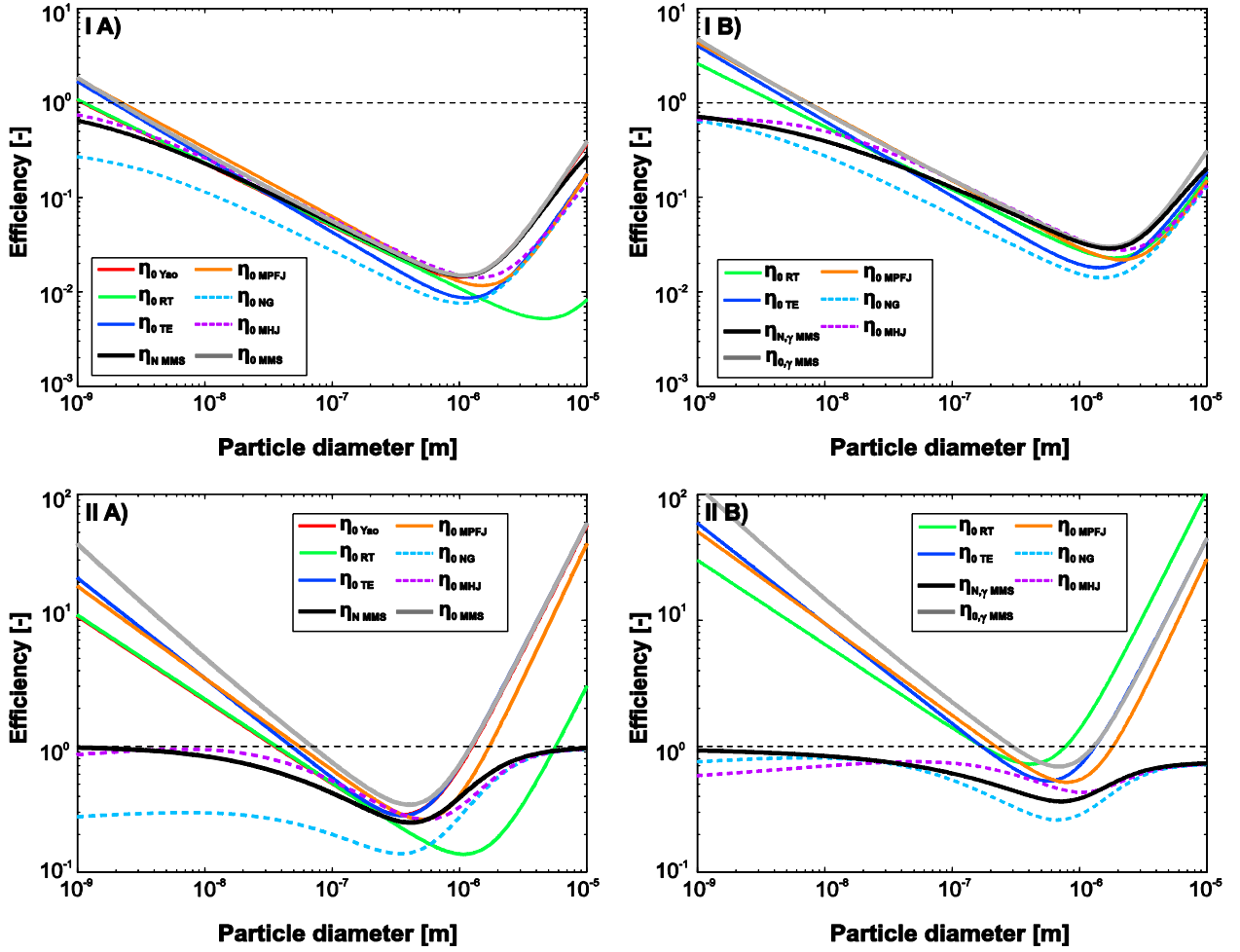

Figure 6: Comparison of the proposed η_N and η_0 equations with existing models. A) Porosity n ≈1, normalization over the collector projection (Eq. 9 and Eq. 10); B) Porosity n < 1, normalization over the fluid envelope of radius b (Eq. 11 and Eq. 12). Data: ρ_f =998 kg/m³, T=288 K, μ =9.8·10⁻⁴ Pa·s. (I) Case study from [30] (n=0.39, a_c =0.2 mm, U=8·10⁻⁶ m/s, ρ_p =1050 kg/m³, T=288 K); (II) Case study from [31] (n=0.35, a_c =0.5 mm, U=10⁻⁷ m/s, ρ_p =1100 kg/m³, T=291 K).
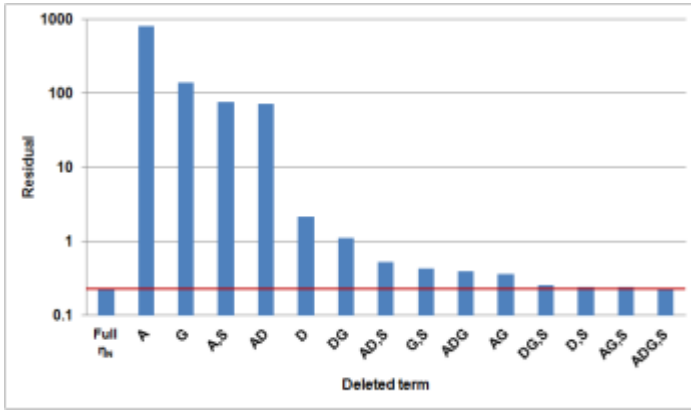
Figure 7: Residual of η_N neglecting the ith term
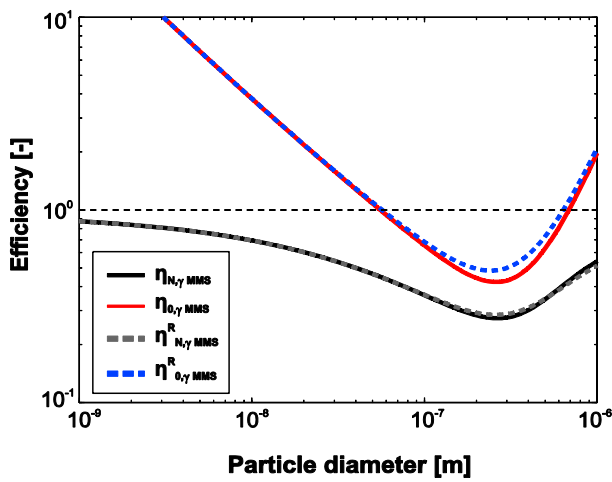

Figure 8: Comparison between the full equations of η_N and η_0 (Eq. 11 and Eq. 12) and the reduced equations (Eq. 13 and Eq. 14). Data: n=0.35, U=10^{-6}m/s, ρ_p =5500 kg/m^3, ρ_f =998 kg/m^3, T=288 K, μ =9.8·10^{-4} Pa·s, a_c =250 µm;

Tables

Table 1: Range of variation of dimensional and non-dimensional parameters. U is the approach velocity (velocity far from the collector), D is the diffusion coefficient, k is the Boltzmann constant, T is the absolute temperature, μ is the water dynamic viscosity, a_p is the particle radius, V is the sedimentation velocity given by the Stokes low [22], ρ_p is the particle density, ρ_f is the fluid density, g is the gravity acceleration vector and a_c is the collector radius

	Parameters	Type of simulations	Values	# Values	Units
Advection	U	Eulerian	$0; 10^{-5}$	2	m/s
		Lagrangian	$0; 10^{-5}$	2	
Diffusion	$D = \dfrac{kT}{6\pi\mu a_p}$	Eulerian	$2.5\cdot10^{-17}; 2.5\cdot10^{-16}; 2.5\cdot10^{-15}; 2.5\cdot10^{-14}; 2.5\cdot10^{-13}; 2.5\cdot10^{-12}; 2.5\cdot10^{-11}; 2.5\cdot10^{-10}; 2.5\cdot10^{-9}; 2.5\cdot10^{-8}$	10	m²/s
		Lagrangian	0	1	
Gravity	$\mathbf{V} = \dfrac{2}{9}\dfrac{a_p^2(\rho_p - \rho_f)}{\mu}\mathbf{g}$	Eulerian	$0; 10^{-9}; 10^{-8}; 10^{-7}; 10^{-6}; 10^{-5}; 10^{-4}; 10^{-3}; 10^{-2}; 10^{-1}; 1$	11	m/s
		Lagrangian	$0; 10^{-9}; 10^{-8}; 10^{-7}; 10^{-6}; 10^{-5}; 10^{-4}; 10^{-3}; 10^{-2}; 10^{-1}; 1$	11	
Particle radius	a_p	Eulerian	$0, 10^{-8}; 10^{-7}; 10^{-6}; 10^{-5}; 10^{-4}$	6	m
		Lagrangian	$0; 5\cdot10^{-9}; 10^{-8}; 5\cdot10^{-8}; 10^{-7}; 5\cdot10^{-7}; 10^{-6}; 5\cdot10^{-6}; 10^{-5}; 10^{-4}$	10	
Peclet number	$N_{Pe} = \dfrac{2a_c U}{D}$	**Eulerian**	**$0, 10^{-1}; 1; 10^1; 10^2; 10^3; 10^4; 10^5; 10^6; 10^7; 10^8$**	**10**	**-**
		Lagrangian	∞	**1**	
Gravity number	$N_G = \dfrac{V}{U}$	**Eulerian**	**$0; 10^{-4}; 10^{-3}; 10^{-2}; 10^{-1}; 1; 10^1; 10^2; 10^3; 10^4; 10^5, \infty$**	**12**	**-**
		Lagrangian	**$0; 10^{-4}; 10^{-3}; 10^{-2}; 10^{-1}; 1; 10^1; 10^2; 10^3; 10^4; 10^5, \infty$**	**12**	
Steric number or Aspect ratio	$N_R = \dfrac{a_p}{a_c}$	**Eulerian**	**$0; 4\cdot10^{-5}; 4\cdot10^{-4}; 4\cdot10^{-3}; 4\cdot10^{-2}; 4\cdot10^{-1}$**	**6**	**-**
		Lagrangian	**$0; 2\cdot10^{-5}; 4\cdot10^{-5}; 2\cdot10^{-4}; 4\cdot10^{-4}; 2\cdot10^{-3}; 4\cdot10^{-3}; 2\cdot10^{-2}; 4\cdot10^{-2}; 4\cdot10^{-1}$**	**10**	

Table 2: Exponents and coefficients for Eq. 6 and Eq. 7. (*) Yao et al.[25] values for the correspondent terms (more significant digits can be found at http://areeweb.polito.it/ricerca/groundwater/software/ETAMMS2015.html).

Parameters			Transport Mechanisms						
			i=1	*i=2*	*i=3*	*i=4*	*i=5*	*i=6*	*i=7*
			Advection (A)	Gravity (G)	Diffusion (D)	A - G	A - D	G - D	A - D - G
Point-particles	**Exponents**	α_i	1 (*1)	0	0	0.1259	0.3662	0	0.1562
		β_i	0	1 (*1)	0	0.8741	0	0.6550	0.5873
		$1-\alpha_i-\beta_i$	0	0	1	0	0.6338 (*2/3)	0.3450	0.2565
	Coefficients	$k_{s1,i}$	0	1 (*1)	7.5609	0.0442	2.9352 (*4.04)	0.9461	-0.6740
		$k_{c1,i}$	1 (*1)	1	7.5609	0.0442	2.9352	2.7972	-1.1945
Steric effect for	**Exponents**	γ_i	1.9834 (*2)	2	1	0.4210	0.3737	0.6012	0.5438

| finite-size particles (S) | Coefficients | $k_{s2,i}$ | 1.5062 (*3/2) | 6.0187 | 4.9534 | 0.1220 | 2.7480 | 1.1626 | -0.7119 |
| | | $k_{c2,i}$ | 6.0098 | 6.0187 | 4.9534 | 0.1220 | 2.7480 | 3.4372 | -1.2616 |

References

[1]   J.F. Mccarthy, J.M. Zachara, Environ Sci Technol 23 (1989) 496.

[2]   J.F. Schijven, G. Medema, A.J. Vogelaar, S.M. Hassanizadeh, J Contam Hydrol 44 (2000) 301.

[3]   J.P. Loveland, S. Bhattacharjee, J.N. Ryan, M. Elimelech, J Contam Hydrol 65 (2003) 161.

[4]   S. Bhattacharjee, J.N. Ryan, M. Elimelech, J Contam Hydrol 57 (2002) 161.

[5]   Y. Liang, S.A. Bradford, J. Simunek, M. Heggen, H. Vereecken, E. Klumpp, Environ Sci Technol 47 (2013) 12229.

[6]   V.I. Syngouna, C.V. Chrysikopoulos, J Contam Hydrol 129 (2012) 11.

[7]   S.A. Bradford, Y.S. Wang, H. Kim, S. Torkzaban, J. Simunek, J Environ Qual 43 (2014) 421.

[8]   N. Seetha, M.S.M. Kumar, S.M. Hassanizadeh, A. Raoof, J Contam Hydrol 164 (2014) 163.

[9]   S. Bensaid, D.L. Marchisio, D. Fino, Chem Eng Sci 65 (2010) 357.

[10]   S. Bensaid, D.L. Marchisio, N. Russo, D. Fino, Catal Today 147 (2009) S295.

[11]   T. Tosco, M.P. Papini, C.C. Viggi, R. Sethi, Journal of Cleaner Production 77 (2014) 10.

[12]   E. Dalla Vecchia, M. Luna, R. Sethi, Environ Sci Technol 43 (2009) 8942.

[13]   S. Comba, D. Dalmazzo, E. Santagata, R. Sethi, J Hazard Mater 185 (2011) 598.

[14]   D. O'Carroll, B. Sleep, M. Krol, H. Boparai, C. Kocur, Adv Water Resour 51 (2013) 104.

[15]   C.M. Kocur, A.I. Chowdhury, N. Sakulchaicharoen, H.K. Boparai, K.P. Weber, P. Sharma, M.M. Krol, L. Austrins, C. Peace, B.E. Sleep, D.M. O'Carroll, Environ Sci Technol 48 (2014) 2862.

[16]   A. Tiraferri, K.L. Chen, R. Sethi, M. Elimelech, Journal of Colloid and Interface Science 324 (2008) 71.

[17]   Q.A. Pankhurst, J. Connolly, S.K. Jones, J. Dobson, J Phys D Appl Phys 36 (2003) R167.

[18]   A.C. Gordon, R.J. Lewandowski, R. Salem, D.E. Day, R.A. Omary, A.C. Larson, J Vasc Interv Radiol 25 (2014) 397.

[19]   X.Y. Shi, M. Prodanovic, J. Holder, K.E. Gray, D. DiCarlo, J Petrol Sci Eng 112 (2013) 88.

[20]   C. O'May, N. Tufenkji, Appl Environ Microb 77 (2011) 3061.

[21]   M.D. Becker, Y. Wang, J. L Paulsen, Y.Q. Song, L.M. Abriola, K.D. Pennell, Nanoscale 7 (2014) 1047.

[22]   C. Tien, B.V. Ramarao, Granular Filtration of Aerosols and Hydrosols. Elsevier 1989.

[23]   M. Elimelech, X. Jia, J. Gregory, R. Williams, Particle Deposition and Aggregation: Measuremen, Modeling and Simulation. Butterworth-Heinemann, 1998.

[24]   A.R. Petosa, D.P. Jaisi, I.R. Quevedo, M. Elimelech, N. Tufenkji, Environ Sci Technol 44 (2010) 6532.

[25]   K.M. Yao, M.M. Habibian, C.R. O'Melia, Environ Sci Technol 5 (1971) 1105.

[26]   V.G. Levich, Physicochemical Hydrodynamics. Prentice-Hall: Englewood Cliffs, NJ, 1962.

[27]   K.M. Yao. Influence of suspended particle size on the transport aspect of water filtration. University of North Carolina at Chapel Hill, 1968.

[28]   R. Rajagopalan, C. Tien, Aiche J 22 (1976) 523.

[29]   J. Happel, Aiche J 4 (1958) 197.

[30]   N. Tufenkji, M. Elimelech, Environ Sci Technol 38 (2004) 529.

[31]   K.E. Nelson, T.R. Ginn, Water Resour Res 47 (2011).

[32]   K.E. Nelson, T.R. Ginn, Langmuir 21 (2005) 2173.

[33]   H. Ma, J. Pedel, P. Fife, W.P. Johnson, (2009).

[34]   G. Boccardo, D.L. Marchisio, R. Sethi, J Colloid Interface Sci 417 (2014) 227.

[35]   L.F. Song, M. Elimelech, Journal of Colloid and Interface Science 153 (1992) 294.

[36]   H.L. Ma, M. Hradisky, W.P. Johnson, Environ Sci Technol 47 (2013) 2272.

[37]   K.E. Nelson, T.R. Ginn, T. Kemai, Environ Sci Technol 47 (2013) 8078.

[38]   Z. Adamczyk, T. Dabros, J. Czarnecki, T.G.M. Vandeven, Adv Colloid Interfac 19 (1983) 183.

[39]   D.C. Prieve, E. Ruckenstein, Aiche J 20 (1974) 1178.

[40]   B.E. Logan, D.G. Jewett, R.G. Arnold, E.J. Bouwer, C.R. O'Melia, J Environ Eng-Asce 121 (1995) 869.